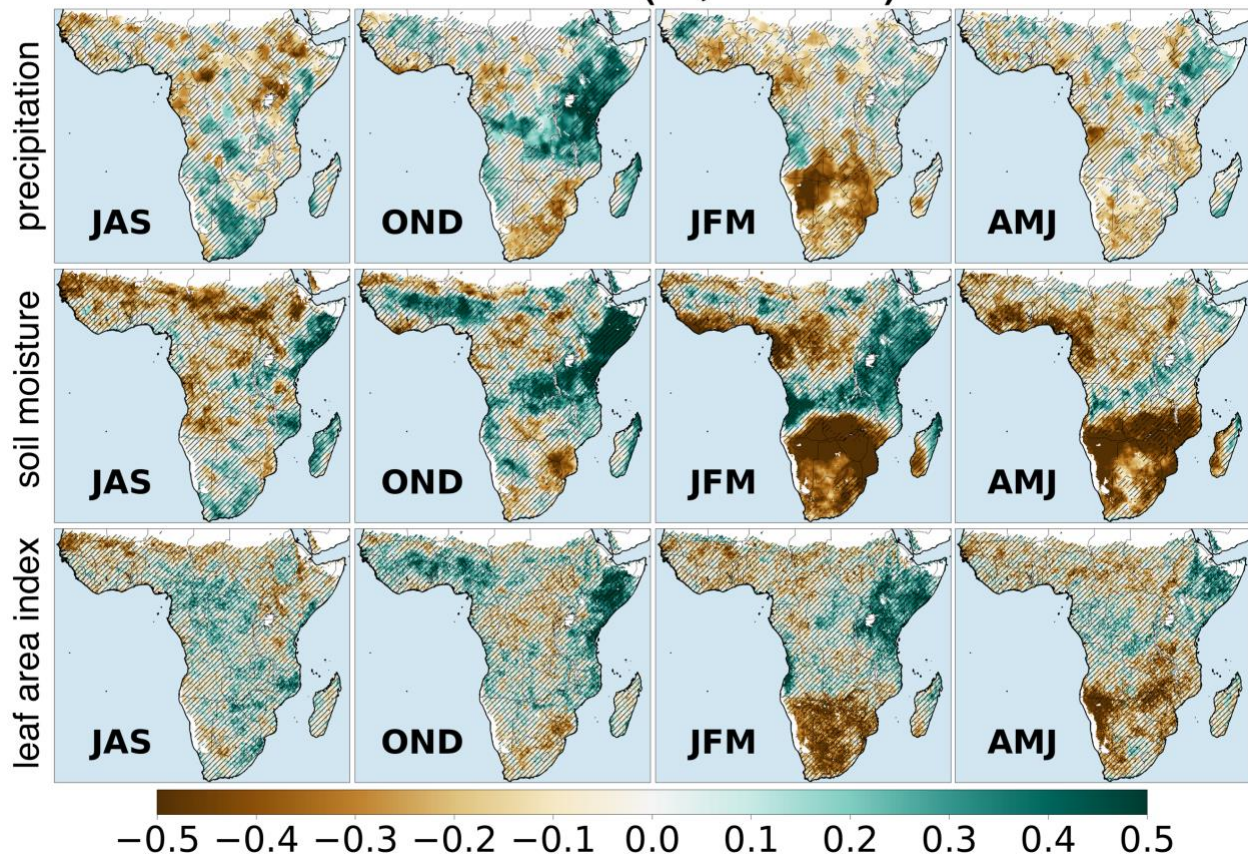


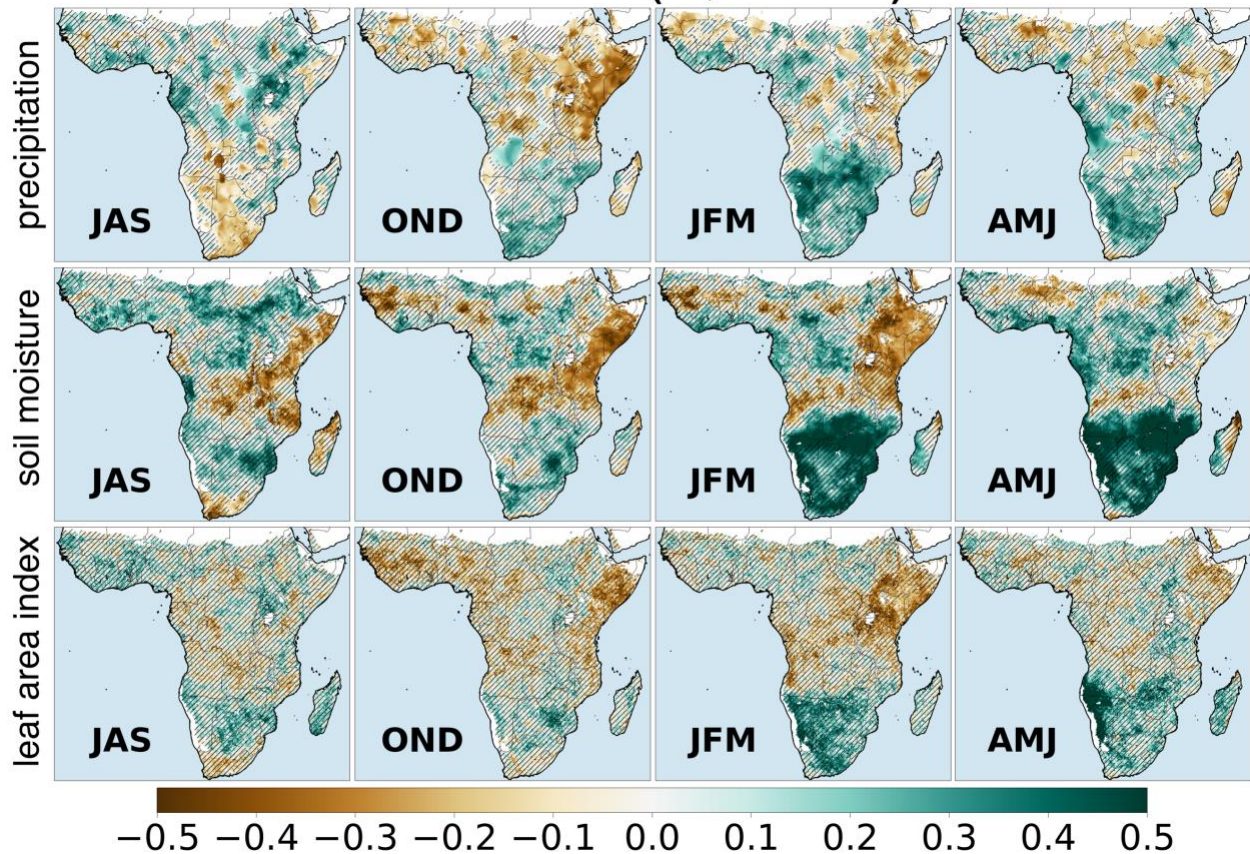
**Supplementary Figure 1.** Maize cropping masks using different coverage thresholds: 0.0%, 0.1%, 1.0%, 2.0%, and 10%. For our analyses of ENSO teleconnections over maize cropping regions, we used the 1.0% masking threshold.

## El Niño ( $\sigma$ , n=14)



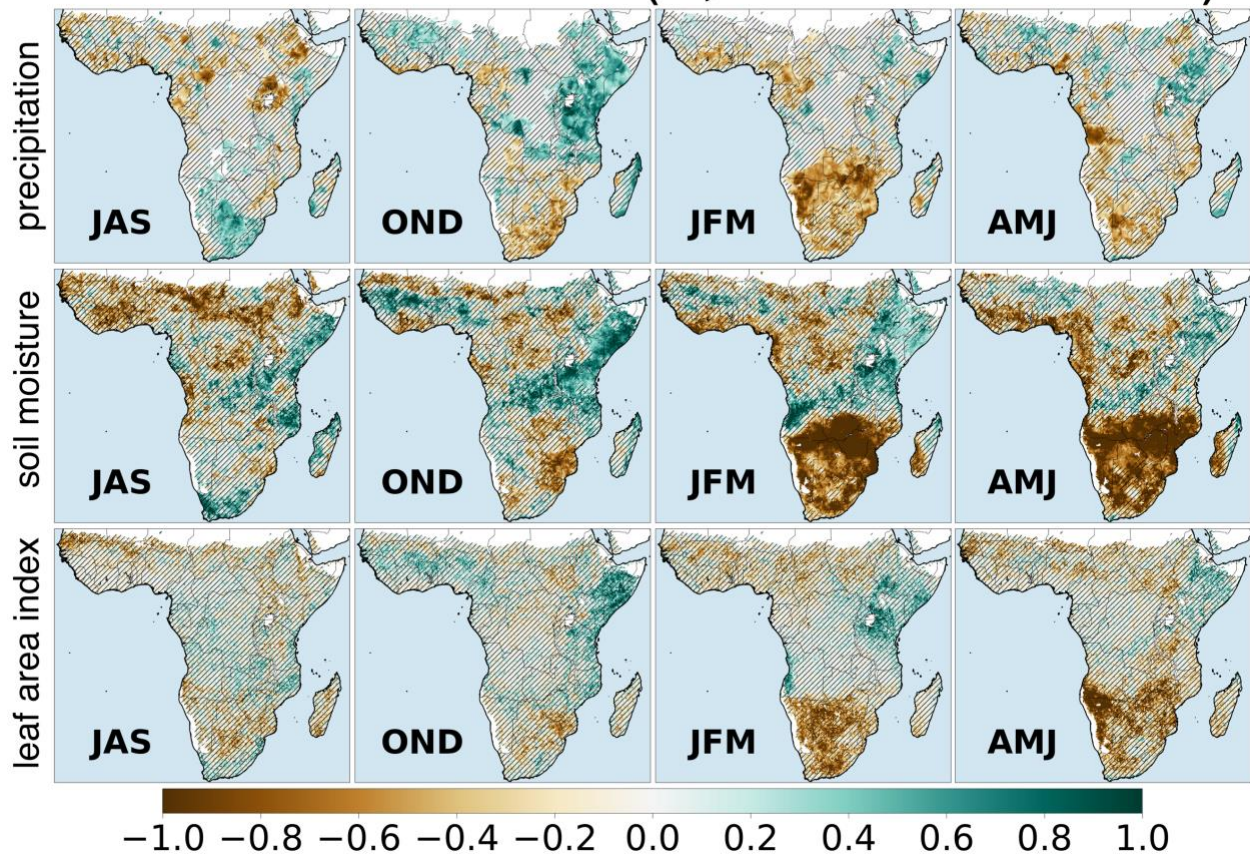
**Supplementary Figure 2.** Composite average standardized anomalies of precipitation, soil moisture (200 cm), and leaf area index during El Niño (n=14) events from 1982—2020 using alternative datasets (GPCC precipitation, GLEAM root zone soil moisture, GIMMS 4g leaf area index). Areas where at least 10 of the 14 (approximately 71%) El Niño events have the same sign of response as the composite average are considered regions with significant agreement in the anomaly sign consensus metric. All other areas are hatched. July-August-September (JAS) and October-November-December (OND) anomalies are taken from the year corresponding with the development of the El Niño event (e.g., 1997), while all other seasons are taken from the following year (e.g., 1998).

## La Niña ( $\sigma$ , n=15)

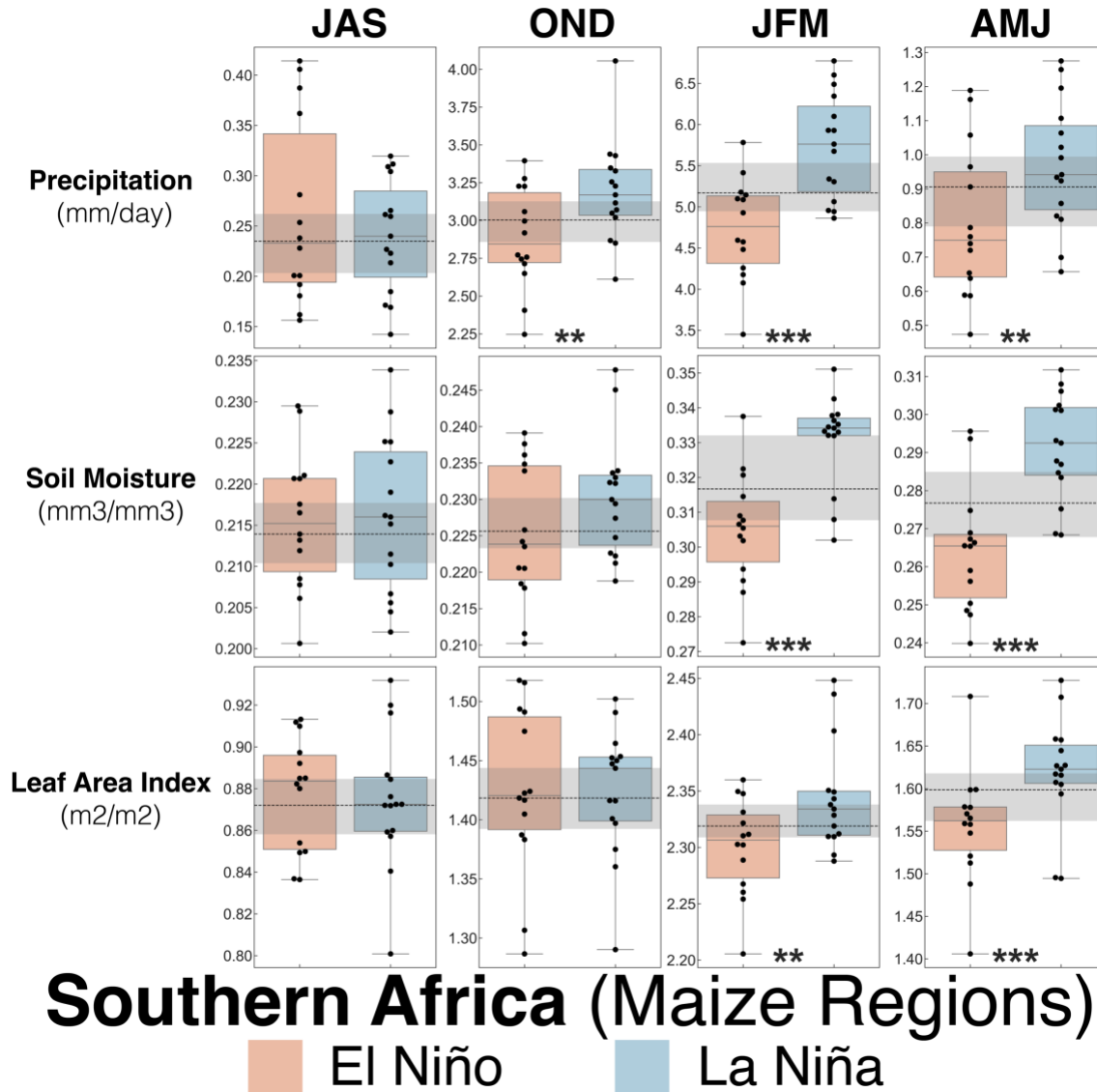


**Supplementary Figure 3.** Composite average standardized anomalies of precipitation, soil moisture (200 cm), and leaf area index during La Niña (n=15) events from 1982—2020 using alternative datasets (GPCP precipitation, GLEAM root zone soil moisture, GIMMS 4g leaf area index). Areas where at least 10 of the 15 (approximately 67%) La Niña events have the same sign of response as the composite average are considered regions with significant agreement in the anomaly sign consensus metric. All other areas are hatched. July-August-September (JAS) and October-November-December (OND) anomalies are taken from the year corresponding with the development of the La Niña event (e.g., 1998), while all other seasons are taken from the following year (e.g., 1999).

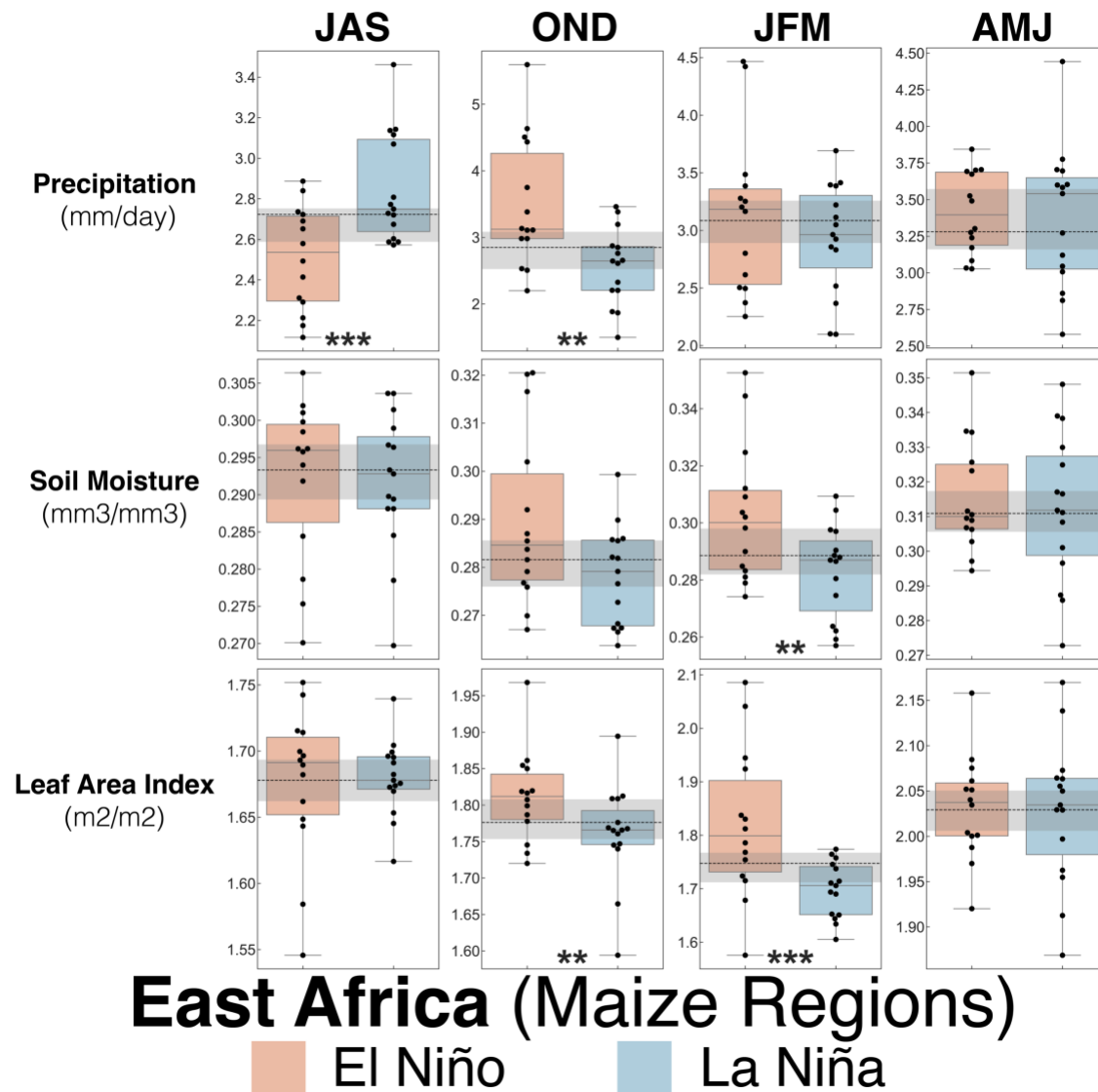
## Median Difference ( $\sigma$ , El Niño-La Niña)



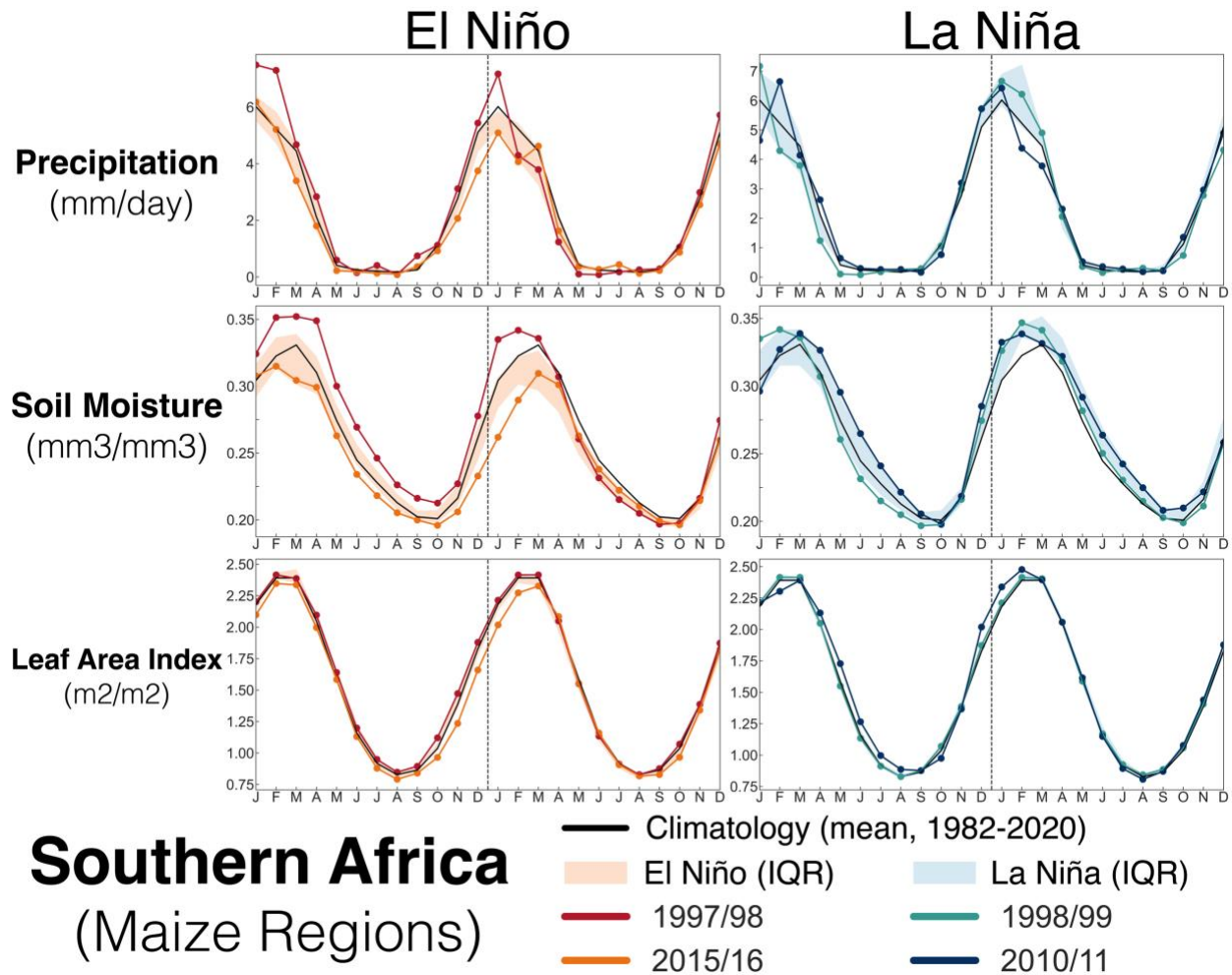
**Supplementary Figure 4.** Differences in median standardized anomalies of precipitation, soil moisture (200 cm), and leaf area index between ENSO phases (El Niño minus La Niña) from 1982—2020 using alternative datasets (GPCP precipitation, GLEAM root zone soil moisture, GIMMS 4g leaf area index). Significance is assessed using a two sample Wilcoxon-Rank sum test (one sided,  $p < 0.05$ ), with insignificant areas indicated by the hatching. July-August-September (JAS) and October-November-December (OND) anomalies are taken from the year corresponding with the development of the El Niño or La Niña event, while all other seasons are taken from the following year.



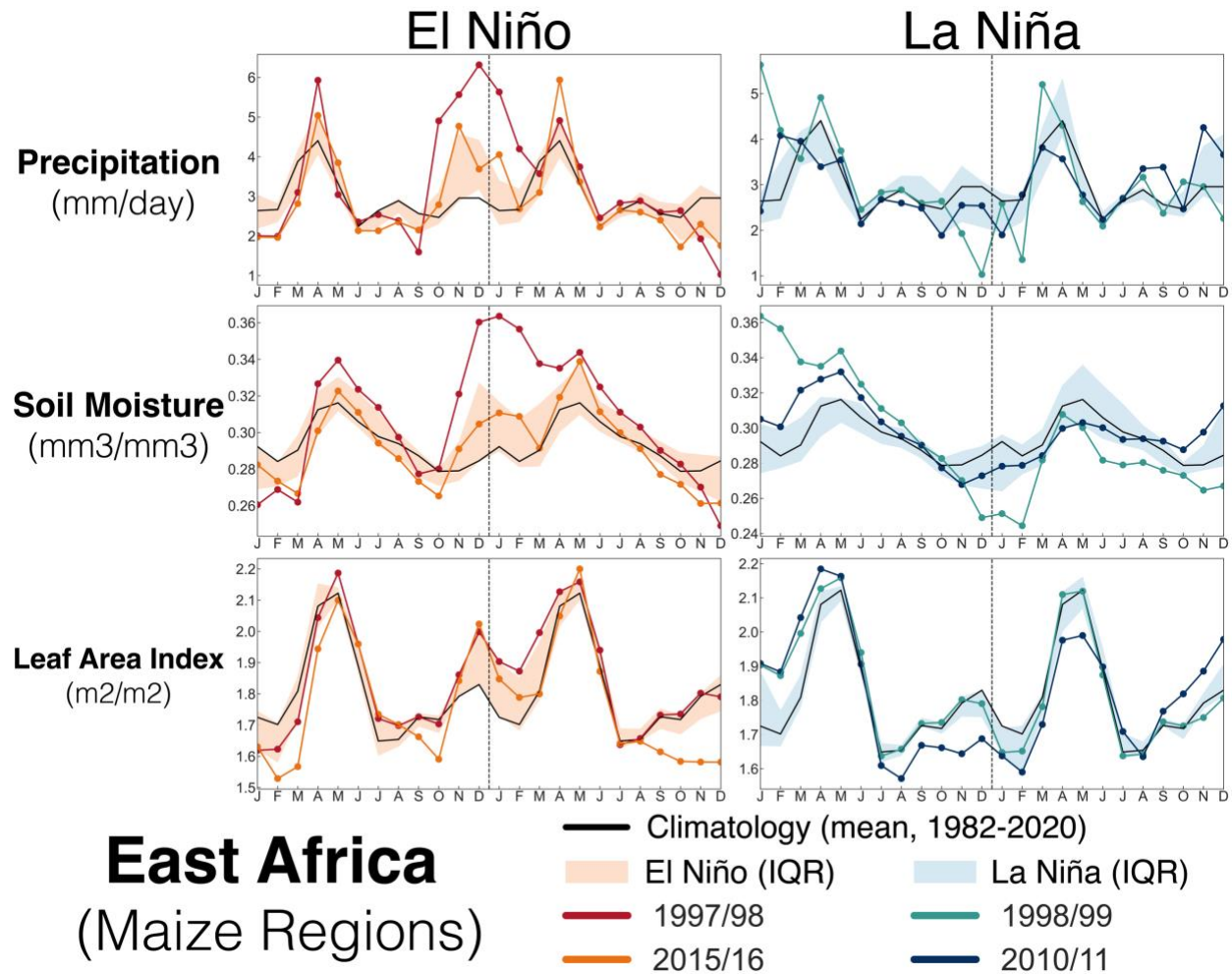
**Supplementary Figure 5.** Box and swarm plots of precipitation, soil moisture (200 cm), and LAI during El Niño and La Niña over southern Africa using alternative datasets (GPCC precipitation, GLEAM root zone soil moisture, GIMMS 4g leaf area index). Each observation is the area-weighted average during the specified season over the maize cropping regions of southern Africa identified in Figure 1. Grey shading indicates the central tercile of anomalies from all years in our datasets (1982--2020). As previously noted, July-August-September (JAS) and October-November-December (OND) anomalies are taken from the year corresponding with the peak in the ENSO event, while other seasons are from the following year. Asterisks indicate significance levels from a two-sample Wilcoxon rank sum test comparing El Niño and La Niña distributions: \* $p \leq 0.10$ , \*\* $p \leq 0.05$ , and  $p \leq 0.01$ .



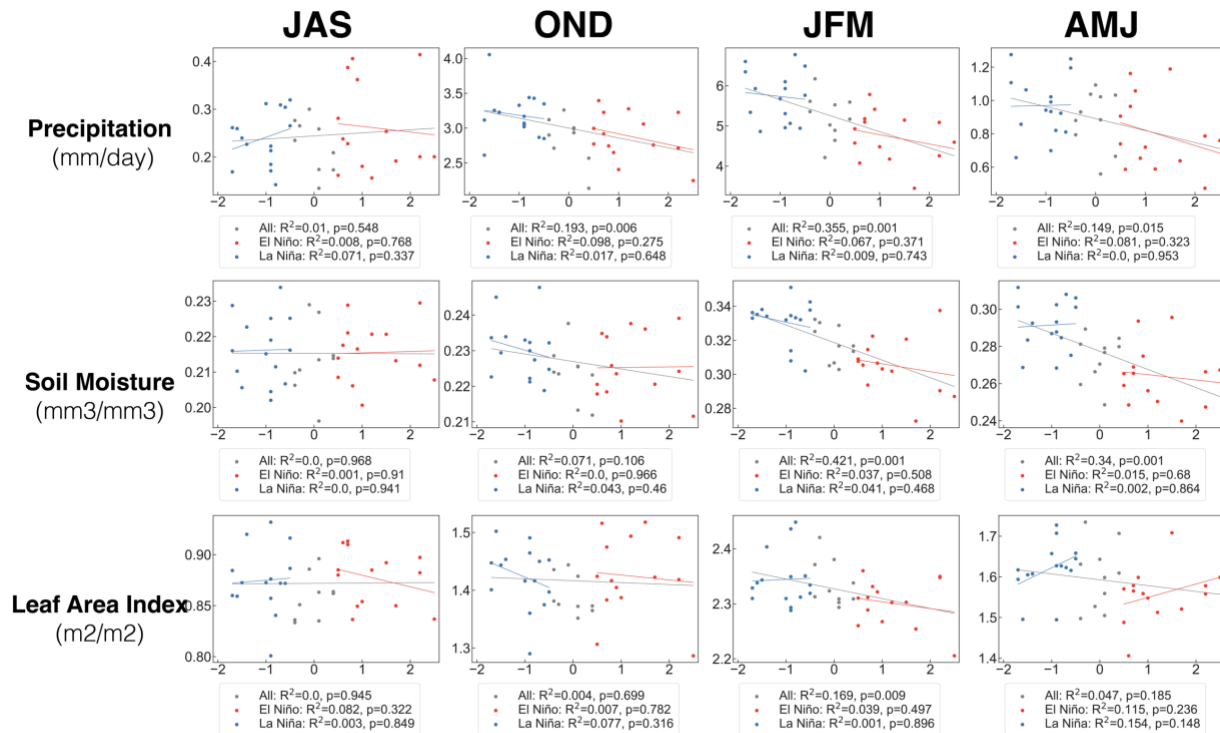
**Supplementary Figure 6.** Box and swarm plots of precipitation, soil moisture (200 cm), and LAI during El Niño and La Niña over East Africa using alternative datasets (GPCP precipitation, GLEAM root zone soil moisture, GIMMS 4g leaf area index). Each observation is the area-weighted average during the specified season over the maize cropping regions of East Africa identified in Figure 1. Grey shading indicates the central tercile of anomalies from all years in our datasets (1982--2020). As previously noted, July-August-September (JAS) and October-November-December (OND) anomalies are taken from the year corresponding with the peak in the ENSO event, while other seasons are from the following year. Asterisks indicate significance levels from a two-sample Wilcoxon rank sum test comparing El Niño and La Niña distributions: \* $p \leq 0.10$ , \*\* $p \leq 0.05$ , and \*\*\* $p \leq 0.01$ .



**Supplementary Figure 7.** Seasonal cycles of precipitation (mm/day), soil moisture (200 cm, mm<sup>3</sup>/mm<sup>3</sup>), and LAI (m<sup>2</sup>/m<sup>2</sup>), averaged over maize cropping regions of southern Africa using alternative datasets (GPCC precipitation, GLEAM root zone soil moisture, GIMMS 4g leaf area index). Mean climatology (1982--2020) is shown in the thin black line. The interquartile ranges for all El Niño and La Niña events are in the red and blue shading, respectively, and individual ENSO events are shown in the colored lines.

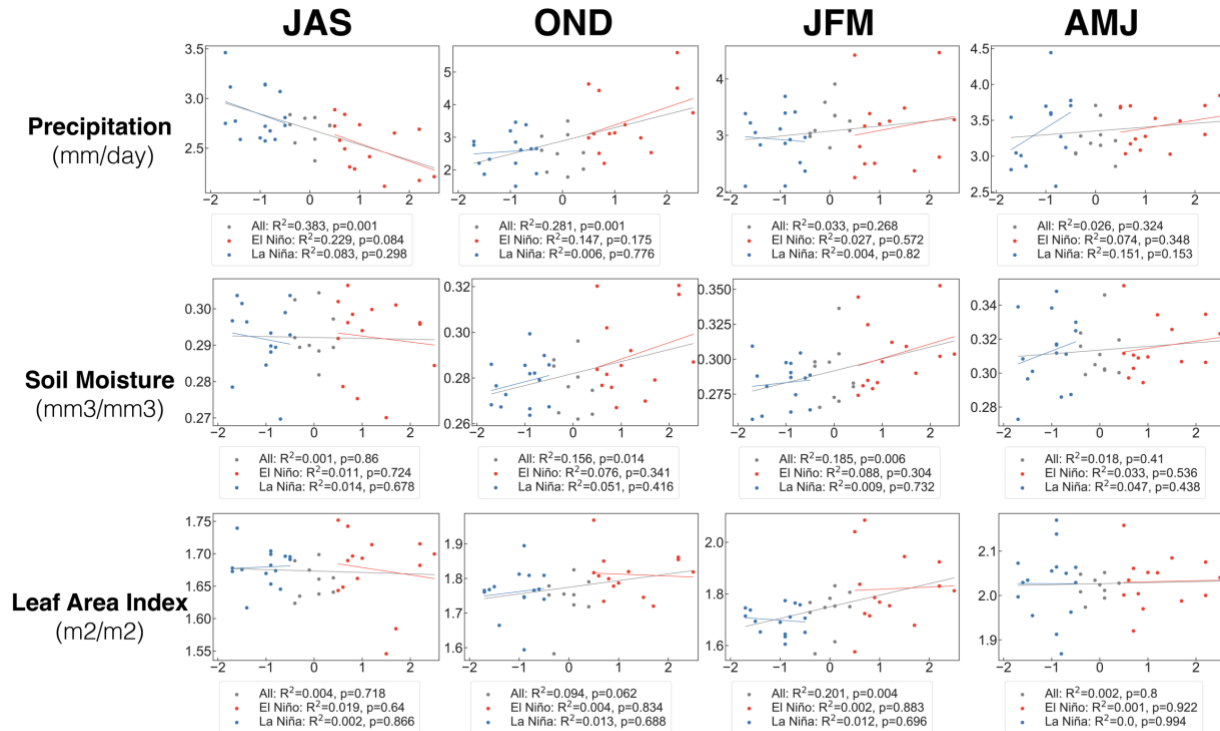


**Supplementary Figure 8.** Seasonal cycles of precipitation (mm/day), soil moisture (200 cm, mm<sup>3</sup>/mm<sup>3</sup>), and LAI (m<sup>2</sup>/m<sup>2</sup>), averaged over maize cropping regions of East Africa using alternative datasets (GPCC precipitation, GLEAM root zone soil moisture, GIMMS 4g leaf area index). Mean climatology (1982--2020) is shown in the thin black line. The interquartile ranges for all El Niño and La Niña events are in the red and blue shading, respectively, and individual ENSO events are shown in the colored lines.



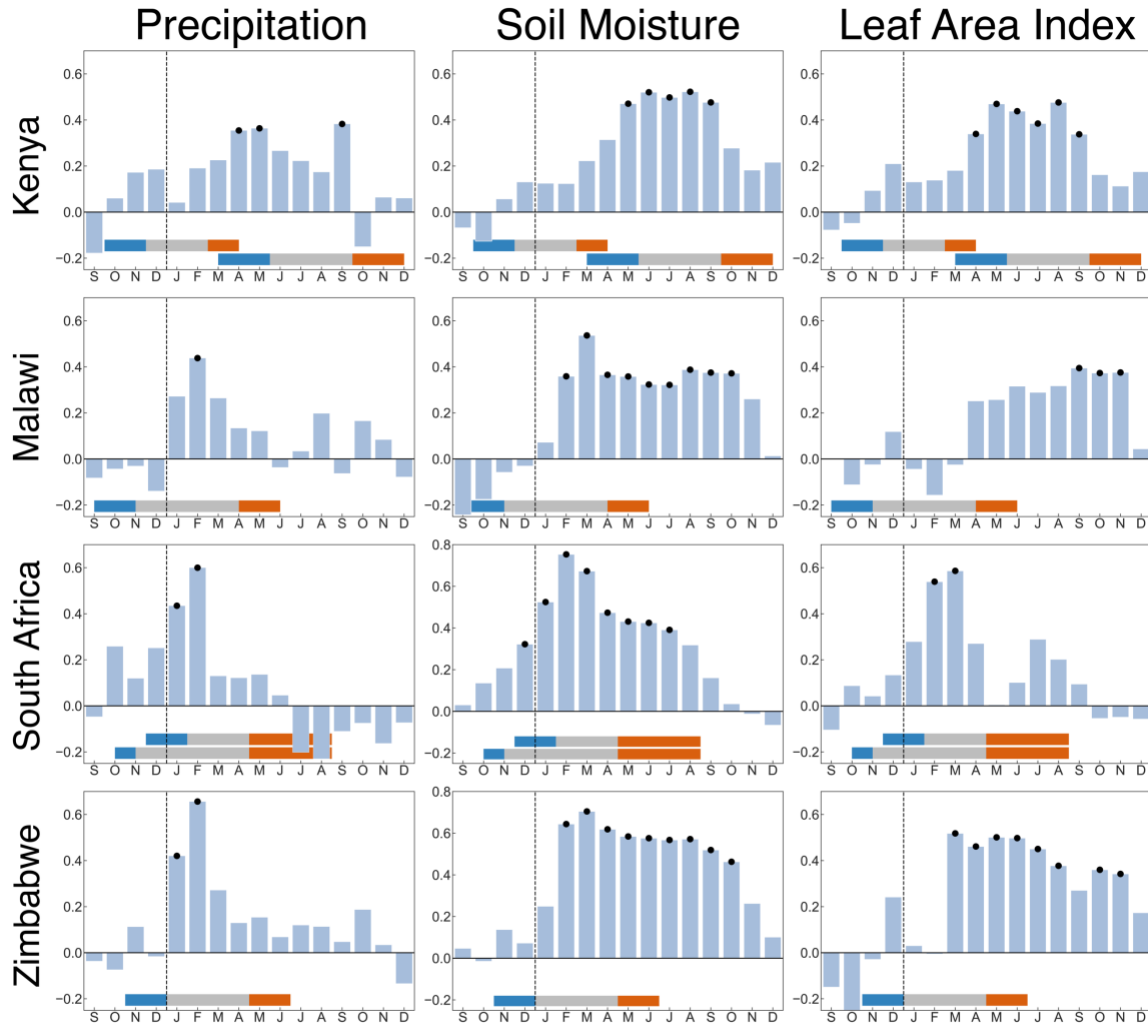
## ENSO in Southern Africa (Maize Regions)

**Supplementary Figure 9.** Scatter plots and regressions between the DJF ONI index and precipitation (mm/day), soil moisture (200 cm, mm<sup>3</sup>/mm<sup>3</sup>), and LAI (m<sup>2</sup>/m<sup>2</sup>), averaged over maize cropping regions of southern Africa using alternative datasets (GPCC precipitation, GLEAM root zone soil moisture, GIMMS 4g leaf area index). Legends display R<sup>2</sup> and significance levels for the regressions using all years (grey lines), El Niño years only (red lines), and La Niña years only (blue lines).



## ENSO in East Africa (Maize Regions)

**Supplementary Figure 10.** Scatter plots and regressions between the DJF ONI index and precipitation (mm/day), soil moisture (200 cm, mm3/mm3), and LAI (m2/m2), averaged over maize cropping regions of East Africa using alternative datasets (GPCC precipitation, GLEAM root zone soil moisture, GIMMS 4g leaf area index). Legends display R<sup>2</sup> and significance levels for the regressions using all years (grey lines), El Niño years only (red lines), and La Niña years only (blue lines).



## Correlations with Crop Yields (Maize Regions)

**Supplementary Figure 11.** Pearson's correlations between country-level maize crop yields and precipitation, soil moisture, and LAI averaged over maize cropping regions within those countries (1983-2020). Correlations were calculated from September of the year prior to harvest (left side of dotted line) through December of the harvest year. Nominally significant correlations ( $n=38$ ,  $p \leq 0.05$ ) are indicated by the black dots. Horizontal shading indicates different phases of the maize growing season: planting (blue), growth (grey), and harvest (orange). Kenya and South Africa have two maize growing seasons. For Kenya, these correspond to the growing season associated with the short (top shading) and long (bottom shading) rains. For South Africa, these different seasons are associated with maize growing in the western (top shading) and eastern (bottom shading) maize regions.